Automated spectral recomposition with application in stratigraphic interpretation[a]

[a]Published in Interpretation, 1, no. 1, SA109-SA116, (2013)

Yihua Cai[*†], *Sergey Fomel*[†], *and Hongliu Zeng*[†]

ABSTRACT

Analyzing seismic attributes in the frequency domain is helpful for reservoir characterization. To analyze the reservoir interval of interest in detail, it is important to capture the seismic response at each frequency subset. Spectral recomposition can be used to extract significant components from the seismic spectrum. We propose a separable nonlinear least-squares algorithm for spectral recomposition, which estimates both linear and nonlinear parts automatically in separate steps. Our approach is applied to estimate fundamental signal parameters, peak frequencies and amplitudes, with which the seismic spectrum can be reconstructed. Automated spectral recomposition helps us visualize frequency-dependent geological features on both cross sections and time slices by extracting significant frequency components. Spectral recomposition can also indicate how frequency contents attenuate with time.

INTRODUCTION

Frequency-domain seismic attributes can be useful in stratigraphic and hydrocarbon reservoir characterization (Castagna et al., 2003; Li et al., 2011). If the seismic response can be captured at each frequency subset, the reservoir interval of interest can then be scrutinized in greater detail. Spectral decomposition is a technique that was developed at Amoco in the 1990's (Partyka et al., 1999). Various time-frequency analysis methods have been employed for frequency decomposition since then. Dilay and Eastwood (1995) applied short-time Fourier transform, which unfortunately suffers from a time-frequency resolution limit (Chakraborty and Okaya, 1995). Liu (2006) and Chen et al. (2008) applied spectral decomposition in the time domain by decomposing the input seismogram into constituent wavelets and then summing the Fourier spectra of individual wavelets. This approach experiences difficulties when the frequency range is large, because it relies on the accuracy of wavelet decomposition, whose residuals commonly introduce bias into "frequency gathers" (Chen et al., 2008). Liu et al. (2011) and Liu (2006) implemented spectral decomposition by time-frequency analysis using an iterative inversion framework with the help of local attributes.

Tomasso et al. (2010) defined *frequency recomposition* in seismic forward modeling as an estimation of components of the seismic spectrum. They showed how to make forward seismic models by recomposing single-frequency models into a multi-frequency model. Different from all previous approaches, spectral recomposition models and reconstructs the seismic spectrum instead of decomposing it. However, Tomasso et al. (2010) manually picked component frequencies and amplitudes, which may not be accurate and highly depends on personal experience. In this paper, we propose spectral recomposition using separable nonlinear least-squares estimation (Golub and Pereyra, 1973), which simultaneously and automatically estimates both linear and nonlinear parts of the Ricker wavelet spectrum. It provides an accurate and direct estimation of amplitudes and peak frequencies of various Ricker wavelets.

A problem is separable if the model can be represented as a linear combination of functions that have a nonlinear parametric dependence. A separable least-squares estimation fits frequencies and amplitudes with large variations, and provides computing confidence, as well as prediction and calibration intervals. The Gauss-Newton algorithm, a method of minimizing the residual sum of squares, is effective both when residuals are small and when measurement errors are additive and the data set is large (Osborne, 2007). An analogous method was used previously by Browaeys and Fomel (2009) for fitting von Kármán distributions, and by Liu and Fomel (2010) for fitting a single Ricker wavelet.

We represent a seismic spectrum as the sum of different Ricker components and use the Gauss-Newton method to fit it with a sum of Ricker wavelet spectra so as to estimate the peak frequency and amplitude of each component. On a field data example from the Gulf of Mexico, we show that automatic spectral recomposition can improve seismic stratigraphic interpretation and help in seismic attribute studies.

THEORY

We represent a seismic spectrum as the sum of different Ricker components (Tomasso et al., 2010):

$$d(f) \approx \sum_{i=1}^{n} a_i \psi_i(m_i, f) \ , \tag{1}$$

where $d(f)$ is the spectrum of a seismic trace, and a_i and m_i are the amplitude and peak frequency of the i-th Ricker spectrum component, given as

$$R(f) = a\,\psi(m, f) = a\,\frac{f^2}{m^2}\,exp(-\frac{f^2}{m^2}) \ . \tag{2}$$

Thus, the model is a linear combination of Ricker wavelet spectra, which has nonlinear functions and depends on multiple parameters. To estimate the Ricker wavelet spectra, we need both $\mathbf{a} = \{a_1, a_2, ..., a_n\}$ and $\mathbf{m} = \{m_1, m_2, ..., m_n\}$ coefficients. The estimation error is

$$r_j = d(f_j) - \sum_{i=1}^{n} a_i(m_i)\psi_i(m_i, f_j) \ . \tag{3}$$

The optimal least-squares estimation requires

$$\min_{\mathbf{a},\mathbf{m}} \|\mathbf{r}(\mathbf{a},\mathbf{m})\|_2^2 \ . \tag{4}$$

The goal of separable nonlinear least-squares estimation (Björck, 1996) is to find a global minimizer of the sum of squares of nonlinear functions. The separability aspect comes from solving linear and nonlinear parts separately (Scolnik, 1972). The algorithm we use in this paper is known as the variable projection algorithm (Golub and Pereyra, 1973). It provides solutions for **a** and **m** by exploring the fact that **r** depends on **a** linearly.

NUMERICAL METHOD

Assuming nonlinear parameters of **m**, linear parameters of **a** can be obtained by solving the linear least-squares problem,

$$\mathbf{a} = \boldsymbol{\psi}(\mathbf{m})^{\dagger}\mathbf{d} \ , \tag{5}$$

where $\boldsymbol{\psi}(\mathbf{m})$ is the matrix composed of $\psi_i(m_i, f_j)$ and $\boldsymbol{\psi}(\mathbf{m})^{\dagger}$ is the Moore-Penrose generalized inverse of the $\boldsymbol{\psi}(\mathbf{m})$ matrix. Replacing this **a** in the original function, the minimization problem takes the form

$$\min_{\mathbf{m}} \left\|(\boldsymbol{I} - \boldsymbol{\psi}(\mathbf{m})\boldsymbol{\psi}(\mathbf{m})^{\dagger})\mathbf{d}\right\|_2^2 \ , \tag{6}$$

where the linear parameters have been eliminated (Golub and Pereyra, 1973). We use the Gauss-Newton method (Björck, 1996) to linearize the problem as follows:

$$\begin{aligned} d(f_i) &\approx \sum_i R_j(m_i, f_j) + \sum_i \frac{\partial R_j}{\partial m_i}\Delta m_i \\ &\approx \sum_i a_i\, \boldsymbol{\psi}(m_i, f_j) + \sum_i [a_i'\, \boldsymbol{\psi}(m_i, f_j) + a_i\, \boldsymbol{\psi}'(m_i, f_j)]\Delta m_i. \end{aligned} \tag{7}$$

Starting with initial values of m_i, we are able to solve for a_i and a_i' using equation 5. Then we solve for the model increment $\Delta\, m_i$. After a number of iterations, summation of $\Delta\, m_i$ converges to the estimated value. The Gauss-Newton method is efficient. In most cases, approximately 20 iterations provide an acceptable convergence. Fitting more component frequencies helps minimize the residual. Geological factors can help the user decide how many components to include in the model. In addition, providing good initial values helps the algorithm avoid being trapped in a local minimum.

APPLICATION

In this section, we show how spectral recomposition can be used in interpretation. First, we test automated spectral recomposition using synthetic and field data. We

then use automated spectral recomposition to simulate and estimate how frequency components attenuate in the subsurface. Finally, we perform thin-bed stratigraphic interpretation using data from Starfak and Tiger Shoal fields of offshore Louisiana.

Synthetic and field data test

To test our method, we generated a wavelet composed of three Ricker wavelets with peak frequencies of 10, 20, and 50 Hz (Figure 1.) Applying a separable nonlinear least-squares estimation, we estimated peak frequencies at 9.999, 19.999, and 49.995 Hz. The residual sum of squares equals approximately 10^{-7} after 50 iterations. The estimation fits the wavelet spectrum accurately, as shown in Figure 1. Generally speaking, the more terms we use to fit the data, the better fitting result we may obtain. However, it is geological reasoning, not statistical factors that determines how many terms should be used in the model. A real data example, shows that spectral recomposition works well for field data (Figure 2). In this case, the estimated peak frequencies are approximately 15 Hz, 31 Hz, and 43 Hz.

Frequency attenuation estimation

Spectral recomposition can be used to indicate how various frequency components attenuate in the subsurface. Different from spectral decomposition, spectral recomposition extracts significant components from seismic data by modeling the spectrum, i.e. fitting spectrum data with summation of Ricker components. With the help of local time-frequency analysis (Liu et al., 2011), we re-composed the spectra of a seismic trace at each time depth. Figure 3 shows recomposition examples at four different time depths. Figure 4 compares our spectral recomposition result with the result of time-frequency analysis. At approximately 1 second, one of the components has a peak frequency as high as 65 Hz. It attenuates gradually to about 8 Hz in 4 seconds. Spectral decomposition indicates information of whole frequency spectrum at each time depth, but provides us no extracted key components. It can be easily found that the spectral recomposition result is consistent with time-frequency analysis result. Thus, spectral recomposition provides information related to any specific layer in which the user might be interested and builds a deeper understanding of seismic attenuation in the subsurface.

Stratigraphic interpretation

Setting the bandwidth for the frequency component ensures an accurate interpretation. Carrying valuable geological information, the main lobe of a wavelet has a finite duration, which means that it covers a certain range in the frequency domain. However, interpreters tend to pick a single frequency with bandpass filtering, which hardly covers the corresponding seismic information because a single frequency appears as

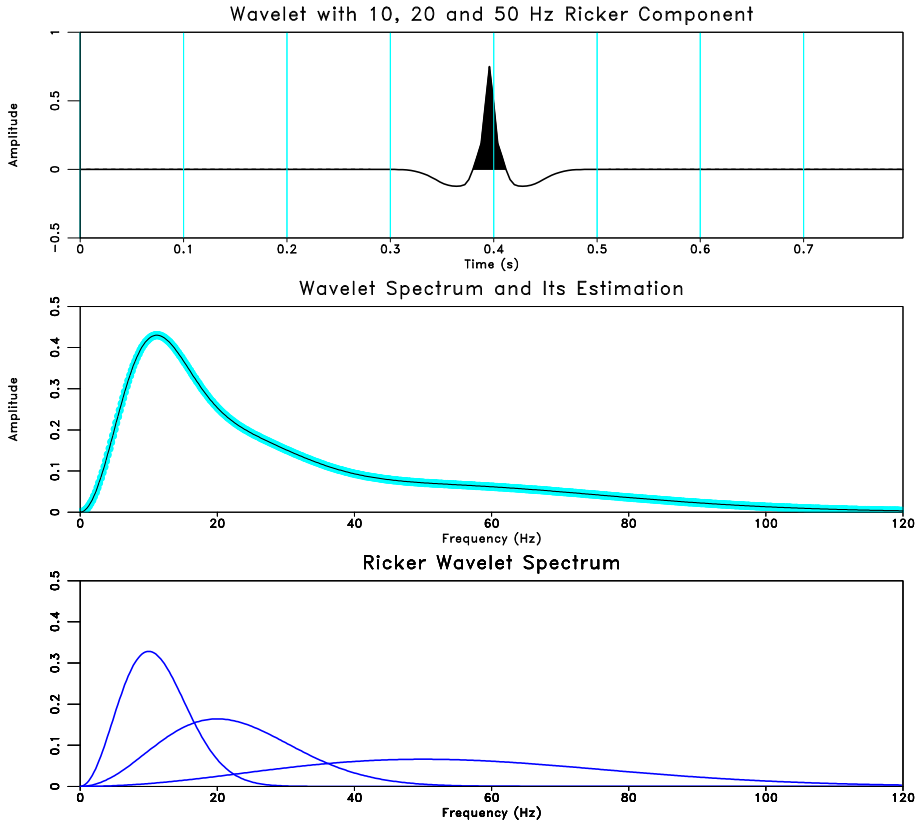

Figure 1: (a) A wavelet composed of 10, 20 and 50 Hz Ricker components. (b) The estimated wavelet spectrum components are plotted individually. The estimated peak frequencies of these components are 9.999, 19.999 and 49.995 Hz. (c) We computed and estimated the spectrum of the wavelet in (a). Spectral recomposition result (in green) fits the spectrum (in black) very well.

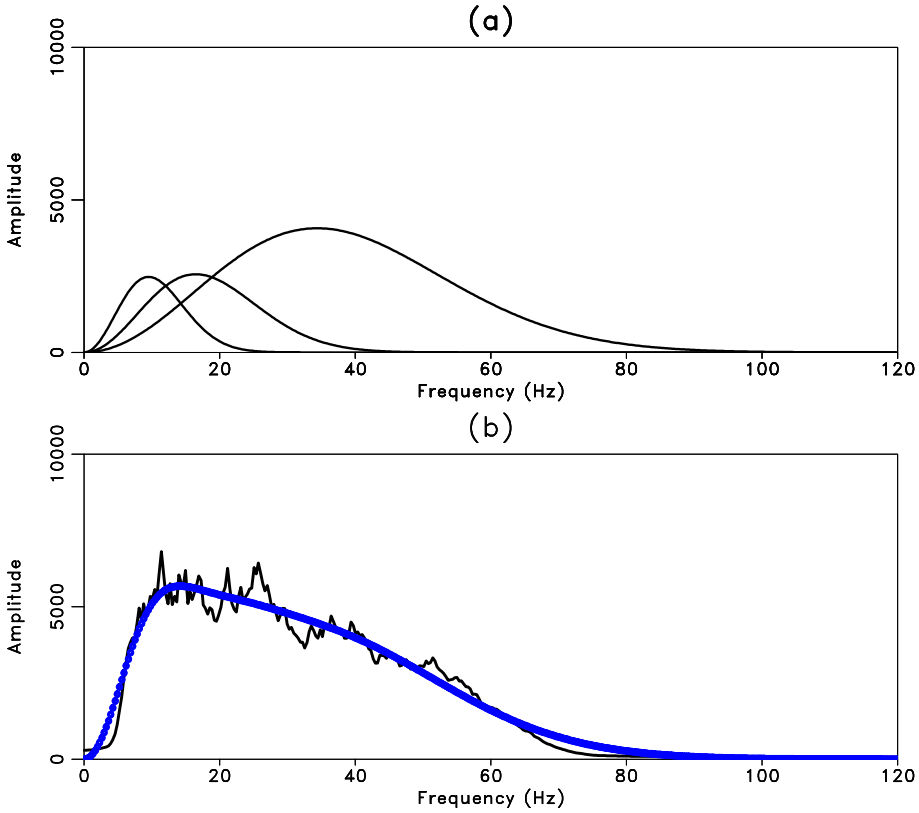

Figure 2: (a) Spectra of ricker wavelet components. Each spectral component is well separated, probably indicating different geological factors. (b) Spectral recomposition result (in blue) fits the seismic spectrum (in black) well.

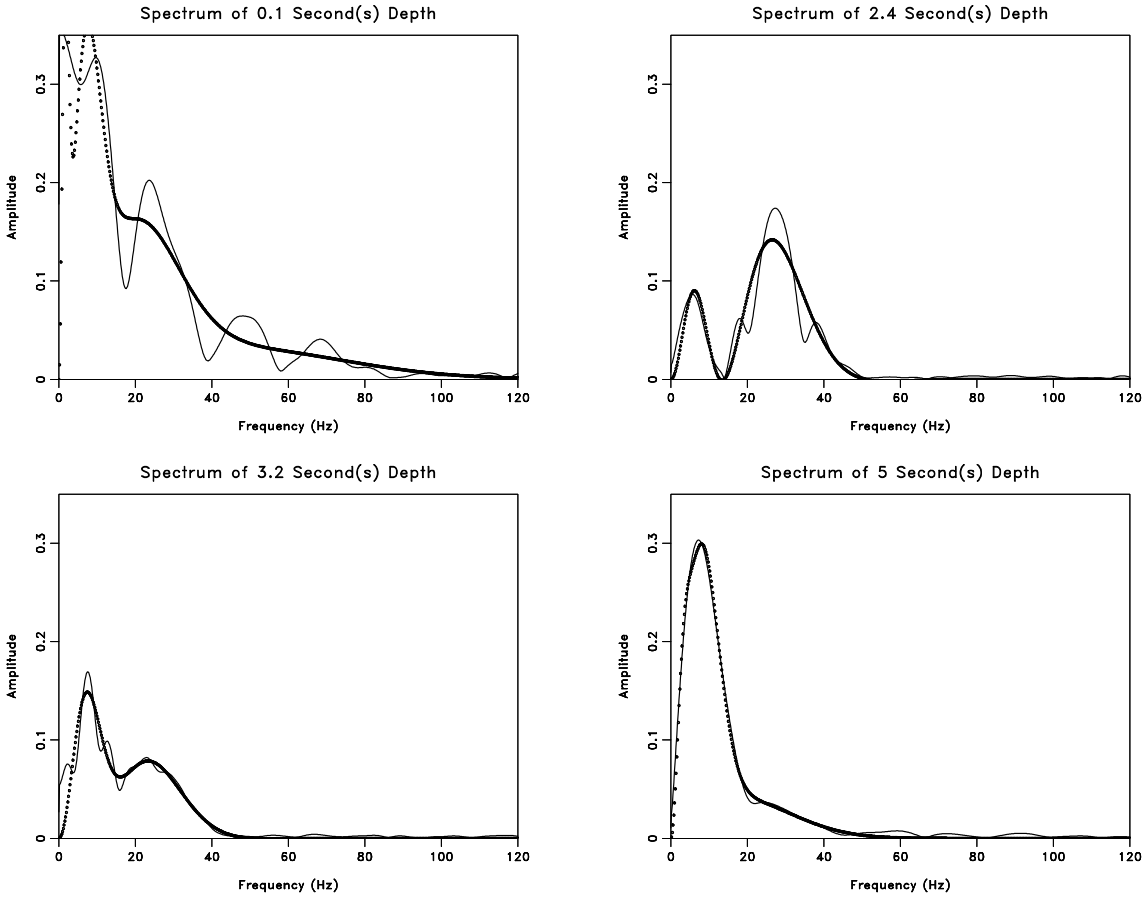

Figure 3: Four time depths, 0, 2, 3 and 5 second have been plotted in (a), (b), (c) and (d) to show spectral recomposition reconstructs Ricker component at different depths. Field data results have been plotted in solid black lines. The spectral recomposition results have been plotted in dotted red lines.

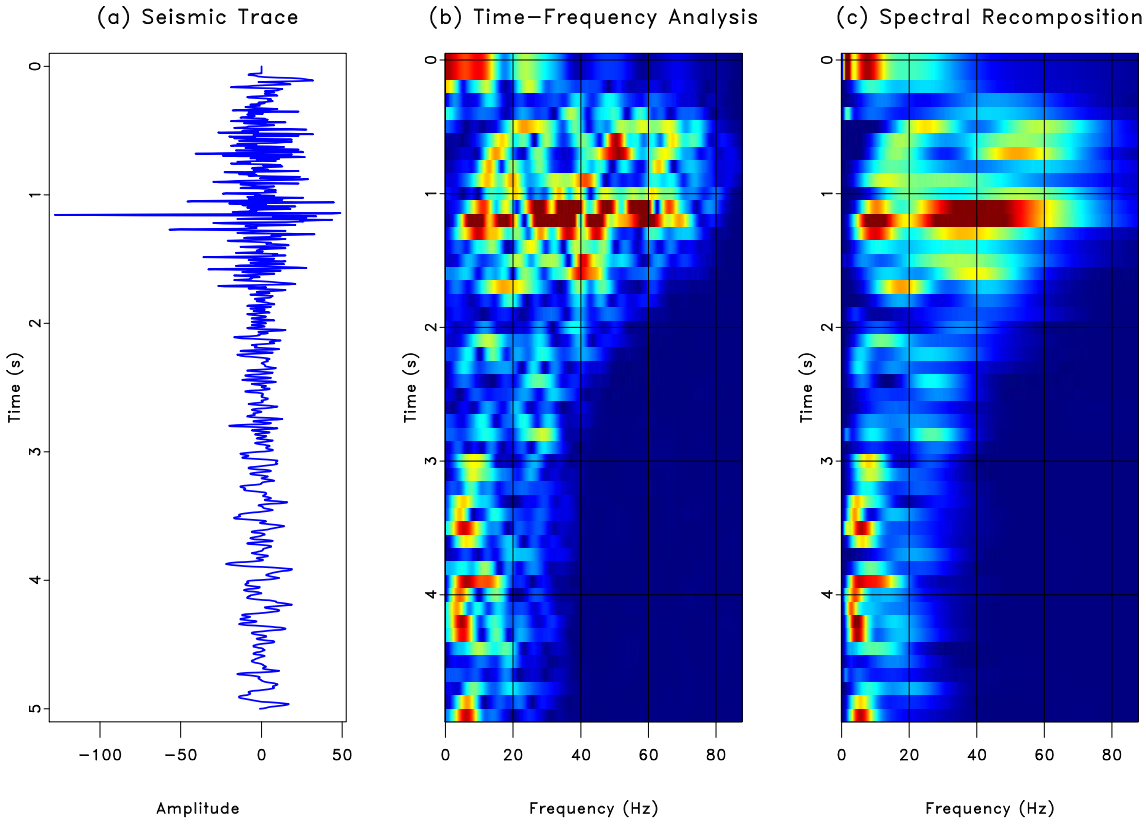

Figure 4: (a) One single seismic trace; (b) Time-frequency analysis result of the trace in (a); (c) Automated spectral recomposition reconstructs Ricker components at each time depth. The reconstructed result is quite consistent with time-frequency analysis in (b).

a spike ignoring all other frequency content. Spectral recomposition helps in computation of frequency bandwidth of the main lobe. One can compute $t_d = \sqrt{6}/(f_m\,\pi)$ as in Figure 5, where t_d is the dominant wavelength and f_m is the peak frequency. The first zero crossing is computed as $t_r = t_d/\sqrt{3}$ (Sheriff, 2002). Having estimated the dominant wavelength, we can set the corresponding bandwidth in the frequency domain.

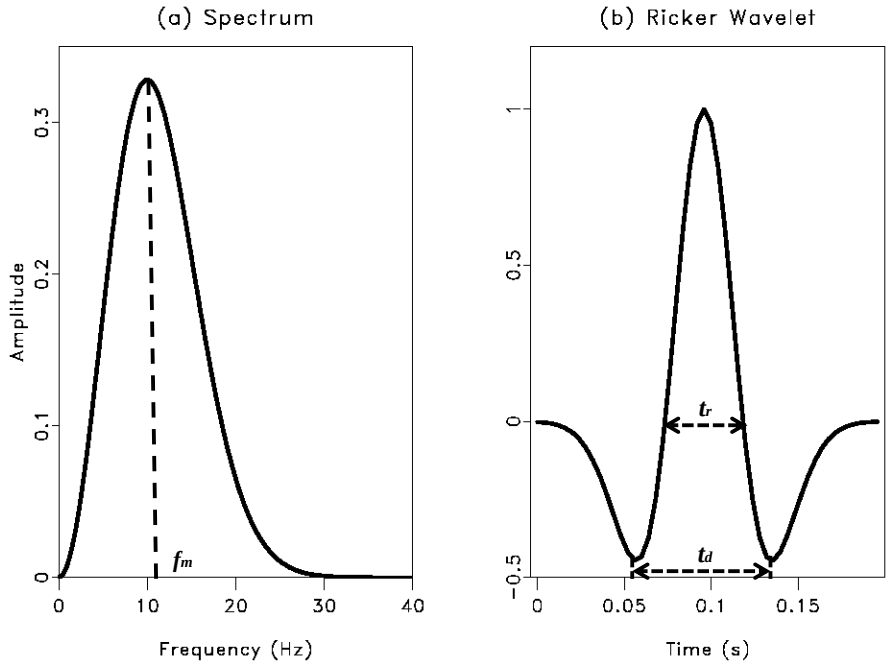

Figure 5: After extracting peak frequency f_m, we compute the dominant wavelength and bandpass filter. (a) Spectrum with peak frequency f_m. (b) Ricker wavelet with dominant wavelength t_d and first zero crossing t_r.

Spectral recomposition extracts significant components from seismic data. Picking the peak frequencies and setting their bandwidths produce results, as shown in Figures 6b and 6c. The same cross section is displayed with a manually picked peak frequency in Figure 6a. Note that Figures 6b and 6c reveal more geologic features. Reflections and seismic events are displayed better in Figure 6b and 6c; for example, a fault system clearly shows up in both Figure 6b and 6c, but not in Figure 6a. Deeper events are also well displayed in Figure 6c, but not in Figure 6a.

The concept behind spectral recomposition is that the seismic response of the geologic unit has a characteristic expression in the frequency domain that is indicative of its significant components (Tomasso et al., 2010). Hence, spectral recomposition can be used in time-slice or stratal-slice interpretation. We start by picking a depositional surface (geologic-time surface) so that any seismic attribute extracted on such a surface could represent a genetic depositional unit. Such a seismic surface display was termed a stratal slice (Zeng et al., 1998a,b). To showcase the "recomposition" technique developed here, we used data from Starfak and Tiger Shoal fields

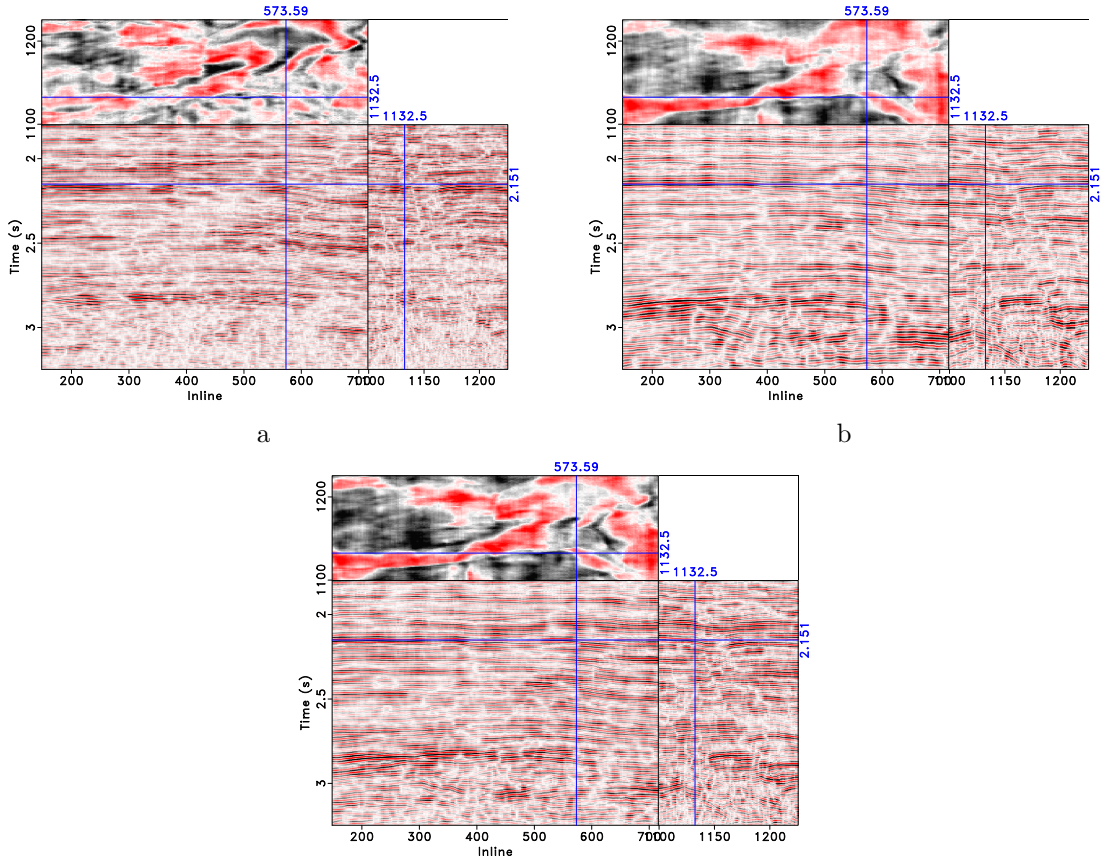

Figure 6: (a) Seismic data from Starfak and Tiger Shoal field displayed with manually picked frequency bandpass filter. Using spectral recomposition, we display the same seismic data with two significant components in (b) and (c). A fault system between inline 800 to 900 clearly stands out in (b). Deep events below 2.4s are well displayed in (c). However, neither the fault system nor the deep events are well displayed in (a).

of offshore Louisiana, a 135-mile^2 3-D survey area. The study area lies along the western periphery of the ancestral Mississippi River depocenter (McGookey, 1975), most recently designated the central Mississippi sediment-dispersal axis by Galloway et al. (2000).

Zeng et al. (2001) constructed and interpreted stratal slices by using special tools to restore and refine multiple seismic slices in the wire-line-log context in both the traveltime domain and the relative geologic-time domain. Their approach includes conditioning seismic data to log lithology by 90^o phasing to achieve better well log integration, imaging, and interpretation of the sequential, planoform geomorphology of the depositional systems (Zeng and Backus, 2005). Our goal is to use spectral recomposition to further improve the image of seismic depositional facies; e.g. a high-frequency component helps indicate thin stratigraphic layers, while a low-frequency component helps identify thick stratigraphic layers. Depositional facies of different thickness can be differentiated using spectral recomposition. After extracting significant spectral components and setting band pass filters, we plotted the stratal slices of Starfak and Tiger Shoal field. Figure 7a is an upper Miocene-age horizon extracted by Zeng and Hentz (2004). Spectral recomposition shows that the component with 22 Hz peak frequency is a significant one, thus we have Figure 7b. As can be seen, Figure 7b improves imaging of the architectural elements within the depositional system. The thin, narrow channel sandstones in relict delta are more clearly imaged in Figure 7b than in Figure 7a. The shelf systems can be easily identified in Figure 7b but not in Figure 7a. Figure 7b is also less affected by acquisition footprint compared with Figure 7a. More than that, spectral recomposition works more efficiently. Both true time and thickness information has been extracted in the process. No prior time or depth-thickness estimate is required for automatic spectral recomposition.

After extracting significant signal components, the result of spectral recomposition naturally admits a Red-Green-Blue (RGB) color-blending plot. RGB color-blending plot takes advantage of the fact that human eyes can discriminate a large numbers of colors. One can plot horizontal slices of different frequency content in different colors, either red, green or blue, and combine them into one figure (Chopra and Marfurt, 2007). Picking frequency subsets automatically with solid geological and geophysical reasoning, spectral recomposition helps standardize the workflow of the RGB color-blending plot. As we have seen in Figure 3, spectral recomposition extracts dominant components at each time depth. Given a time slice or stratal slice, we extract the significant frequency components, compute the duration of the main lope of the wavelet from the area of interest, and set the appropriate bandwidth in the frequency domain. Plotting three different frequency components in RGB colors and combining them together, we produce RGB color-blending plots in Figure 8. With a sense of relative sandstone thickness distribution, RGB color blending of spectral recomposition brings useful information together and helps reveal geological features of interest.

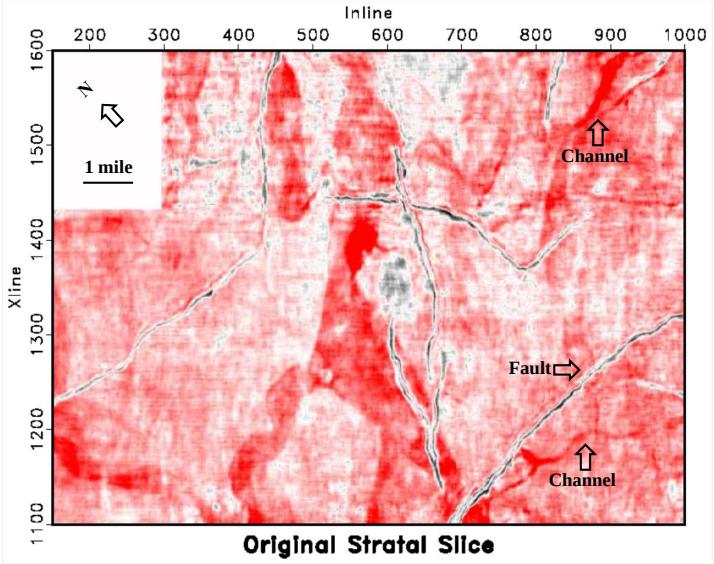

a

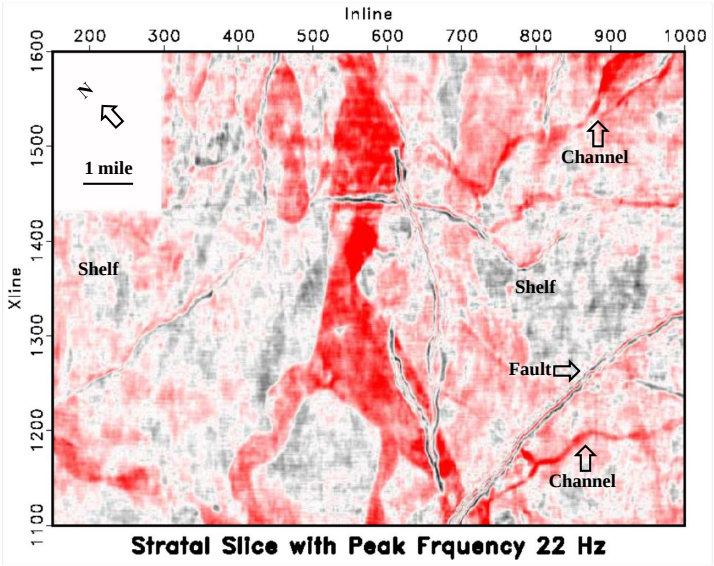

b

Figure 7: Use of spectrum recomposition to improve thin-bed stratigraphic interpretation in Miocene, Starfak-Tiger Shoal fields, offshore Louisiana. (a) A stratal slice made by Zeng et al. (2001). (b) Same stratal slice extracted from 22 Hz component of seismic data.

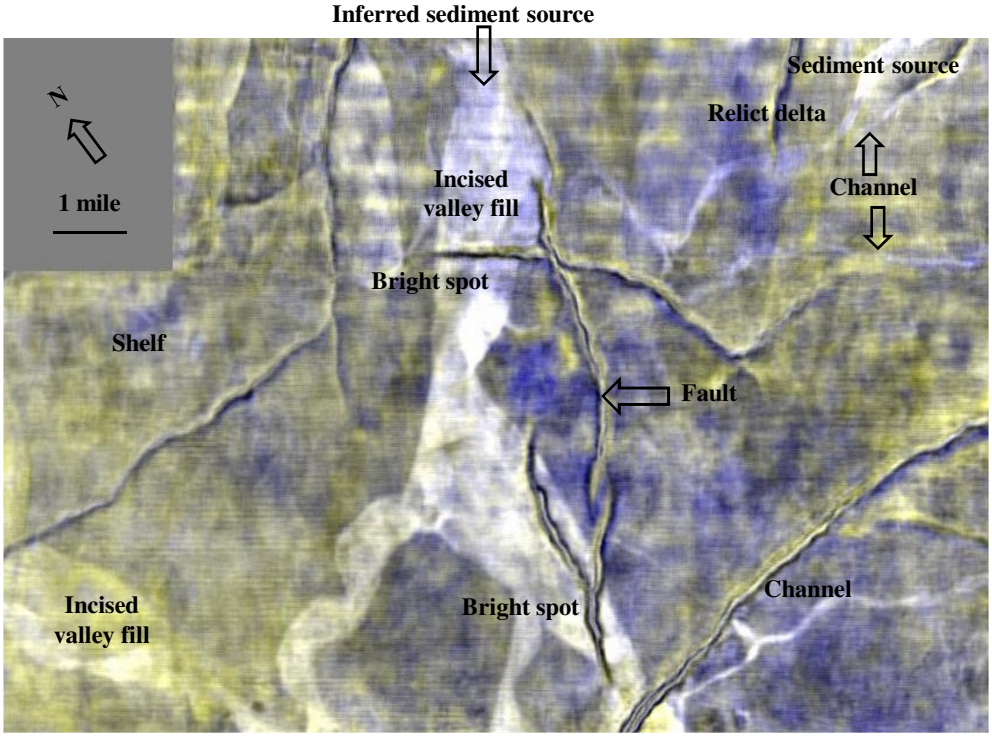

Figure 8: Components of 15, 22, and 29 Hz of Starfak-Tiger Shoal stratal slice picked and plotted using color blending, which provides more detailed information. White bright colors indicate thicker sands; white dim colors refer to thinner sands; blue and dark colors indicate shale. Interpreters can easily identify different depositional facies in plot.

CONCLUSION

Automated spectral recomposition using separable nonlinear least squares represents the seismic spectrum as a sum of Ricker components and efficiently estimates their peak frequencies and amplitudes. With the seismic spectrum reconstructed from component frequencies, spectral recomposition can be used in seismic interpretation. We adopted Ricker wavelet in the analysis because of its popularity. Other wavelets may also be used with corresponding estimation numerical strategy.

Applying spectral recomposition, we have been able to better visualize seismic images in both cross sections and stratal slices. This technique has improved the interpreter's ability to image the various elements of the depositional system in extracted stratal slices. Spectral recomposition can also be used in forward modeling, in studying how different frequency components attenuate in the subsurface, newand in estimating thin-bed thicknesses using tuning frequencies. It provides a robust and phase-independent approach to seismic thickness estimation. Compared with conventional methods involving adjacent peaks and troughs picking, spectral recomposition requires only peak-frequency and amplitude estimation.

ACKNOWLEDGEMENT

We thank Chevron for the seismic data and the Madagascar development community for developing the software used in this paper. Publication is authorized by the Director, Bureau of Economic Geology.

REFERENCES

Björck, Å., 1996, Numerical Methods for Least Squares Problems: Society for Industrial and Applied Mathematics.

Browaeys, T. J., and S. Fomel, 2009, Fractal heterogeneities in sonic logs and low-frequency scattering attenuation: Geophysics, **74**, WA77–WA92.

Castagna, J. P., S. Sun, and R. W. Siegfried, 2003, Instantaneous spectral analysis: Detection of low-frequency shadows associated with hydrocarbons: The Leading Edge, **22**, 120–127.

Chakraborty, A., and D. Okaya, 1995, Frequency-time decomposition of seismic data using wavelet-based methods: Geophysics, **60**, 1906–1916.

Chen, G., G. Matteucci, B. Fahmy, and C. Finn, 2008, Spectral-decomposition response to reservoir fluids from a deepwater West Africa reservoir: Geophysics, **73**, C23–C30.

Chopra, S., and K. Marfurt, 2007, Seismic attributes for prospect identification and reservoir characterization: Society of Exploration Geophysicists.

Dilay, A., and J. Eastwood, 1995, Spectral analysis applied to seismic monitoring of thermal recovering: The Leading Edge, **14**, 1117–1122.

Galloway, W. E., P. E. Ganey-Curry, X. Li, and R. T. Buffler, 2000, Cenozoic depositional history of the Gulf of Mexico Basin: AAPG Bulletin, **84**, 1743–1774.

Golub, G. H., and V. Pereyra, 1973, The differentiation of pseudo-inverses and nonlinear least squares problems whose variables separate: Numerical Analysis, **10**, 413–432.

Li, Y., X. Zheng, and Y. Zhang, 2011, High-frequency anomalies in carbonate reservoir characterization using spectral decomposition: Geophysics, **76**, V47–V57.

Liu, G., S. Fomel, and X. Chen, 2011, Time-frequency analysis of seismic data using local attributes: Geophysics, **76**, P23–P34.

Liu, J., 2006, Spectral Decomposition and Its Application in Mapping Stratigraphy and Hydrocarbons: PhD thesis, Univeristy of Houston.

Liu, Y., and S. Fomel, 2010, Local time-frequency transform and its application to ground-roll noise attenuation, *in* 80th Annual International Meeting: Society of Exploration Geophysicists, 3711–3716.

McGookey, D. P., 1975, Gulf coast cenozoic sediments and structures: An excellent example of extra-continental sedimentation: Gulf Coast Association of Geological Societies Transactions, **25**, 104–120.

Osborne, M. R., 2007, Separable least squares, variable projection, and the Gauss-Newton algorithm: Electronic Transactions on Numerical Analysis, **28**, 1–15.

Partyka, G. J., J. Gridley, and J. Lopez, 1999, Interpretational applications of spectral decomposition in reservior characterization: The Leading Edge, **18**, 353–360.

Scolnik, H. D., 1972, On the solution of non-linear least squares problems: IFIP Congress, IFIP Congress, 1258–1265.

Sheriff, R., 2002, Encyclopedic Dictionary of Applied Geophysics: Soc. Expl. Geophys.

Tomasso, M., R. Bouroullec, and D. R. Pyles, 2010, The use of spectral recomposition in tailored forward seismic modeling of outcrop analogs: AAPG Bulletin, **94**, 457–474.

Zeng, H., and M. M. Backus, 2005, Interpretive advantages of 90°-phase wavelets. Part 1: Modeling: Geophysics, **70**, C7–C15.

Zeng, H., M. M. Backus, K. T. Barrow, and N. Tyler, 1998a, Stratal slicing, part I: Realistic 3-D seismic model: Geophysics, **63**, 502–513.

Zeng, H., S. C. Henry, and J. P. Riola, 1998b, Stratal slicing, part II: Real 3-D seismic data: Geophysics, **63**, 514–522.

Zeng, H., and T. F. Hentz, 2004, High-frequency sequence stratigraphy from seismic sedimentology: Applied to Miocene, Vermilion Block 50, Tiger Shoal area, offshore Louisiana: AAPG Bulletin, **88**, 153–174.

Zeng, H., T. F. Hentz, and L. W. Wood, 2001, Stratal slicing of Miocene-Pliocene sediments in Vermilion Block 50-Tiger Shoal area, offshore Louisiana: the Leading Edge, **20**, 408–418.